Force Prediction in Thread Milling

A. C. Araujo and J. L. Silveira
Department of Mechanical Engineering
EE & COPPE - UFRJ
P.O. Box 68503
21945-970 Rio de Janeiro, RJ. Brazil
anna@ufrj.br
jluis@ufrj.br

S. Kapoor
Department of Mechanical and Industrial Engineering
UIUC - Urbana IL 61801. USA
s-kapoor@uiuc.edu

A mechanistic approach for modeling the thread milling process is presented. The mechanics of cutting for thread milling is analyzed as an end milling process with modified cutting edge. The geometry of threads is added to the geometry of the end milling tool to calculate the chip load area. The linear path is simulated and values of the specific energy from end milling are used to compute the cutting forces involved. A comparison between the simulation of the cutting forces for a specific tool in two different situations is made to present the force behavior acquired from the model.
***Keywords**: Thread milling, mechanistic models, force prediction*

Introduction

Threading a workpiece is a fundamental metalworking process. Threads can be produced in a variety of ways, involving two basic methods: plastic deformation working or metal cutting. The dominant method used in industry is plastic deformation working. Conventional bolts and screws, for example, are mostly made by this method. Threads produced by plastic deformation are stronger because of the grain structure than those produced by cutting, although forming cannot achieve the high accuracy and precision required in many applications. Threads made of brittle materials also cannot be produced by plastic deformation working. In such cases, thread cutting is necessary (Smith, 1989). The common cutting processes for producing internal threads are tapping and thread milling (Stephenson and Agapiou, 1996). Tapping is used to make internal threads with the same diameter of the tool. It is done by feeding the cutting tool into the hole until the desired thread depth is achieved, then reversing the tap to back it out of the hole and remove it from the workpiece. Thread milling tools can produce internal threads with any diameter bigger than the tool diameter as well as external threads. In thread milling, the machine tool executes the thread in one single pass. The tool goes down to the hole and begins the cutting from the deepest part to the top in a helical path, or it begins at the top and goes until the end of the hole. Some geometries of thread milling tools can be observed in Fig. 1. Figure 1a shows a single cutting edge which produces one pitch per feed rotation, Fig. 1b presents a single straight tool with only one cutting edge and Fig. 1c shows a helical thread tool with some cutting flutes. In thread milling high tool pressure are generated which can result into an excessive tool deflection and tool breakage when milling at full thread.

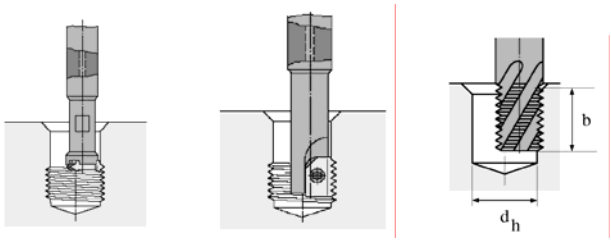

Figure 1. Thread milling tools (a) Single cutting edge, (b) Single straight thread flute, (c) Helical thread flute (Emuge, 2002).

Many authors developed models for prediction of forces in machining. These include analytical, experimental, mechanistic and numerical methods (Ehmann et al., 1997). In thread cutting by tapping, a mechanistic method for the prediction of forces was presented by Dogra et al. (2002). A number of papers describing the thread milling operation have been published (Smith, 1989, Koelsch, 1995, Stephenson and Agapiou, 1996) but there is no model to predict the forces involved in the process.

The objective of this article is to present a mechanistic model for thread milling. The tool geometry analyzed involves triangular and metric threads. The thread milling tool in this article has helical flutes and its geometry is analyzed as a modified end milling tool. Tool run out is added to the model and some examples of thread milling processes are presented.

Nomenclature

d_e = external tool diameter, mm
d_i = internal tool diameter, mm
d_E = external workpiece diameter, mm
d_I = internal workpiece diameter, mm
d_h = hole diameter, mm
d(z) = local diameter, mm
e = width of cut, mm
f_t = feed per tooth, mm
H = thread height, mm
K_n = normal specific cutting pressure, N/mm^2
K_f = radial specific cutting pressure, N/mm^2
K_z = axial specific cutting pressure, N/mm^2
N_f = number of flutes
p = thread pitch, mm
t_c = chip thickness, mm
V_c = cutting speed, m/min

Presented at COBEF 2003 – II Brazilian Manufacturing Congress, 18-21 May 2003, Uberlândia, MG. Brazil.
Paper accepted October, 2003. Technical Editor: Alisson Rocha Machado.

Greek Symbols

α = rake angle, deg.
δ = angle for the total engagement of a cutting edge, deg.
ζ = angle between the flutes, deg.
λ = helix angle, deg.
ξ = thread angle, deg.
φ_1 = initial angle of contact
φ_2 = final angle of contact
ϕ = angular position of a point in a flute
ψ = angular position of the leading point of the cutting edge

Subscripts

e relative to external tool diameter
E relative to external workpiece diameter
i relative to internal tool diameter
I relative to internal workpiece diameter
f,n,z relative to the tool referential
x,y,z relative to the workpiece referential

Thread Milling Geometry

Tool Geometry

The threads studied in this article are metric and triangular. The thread variables presented in Fig. 2a are: thread pitch, p, thread angle, ξ, external workpiece diameter, d_E, internal workpiece diameter, d_I, and thread height H.

The relation between the diameters can be written as:

$$d_I = d_E - \frac{p}{\tan(\xi/2)} \tag{1}$$

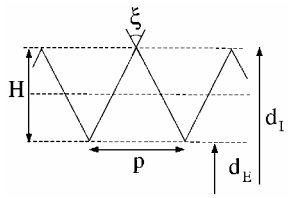

(a)

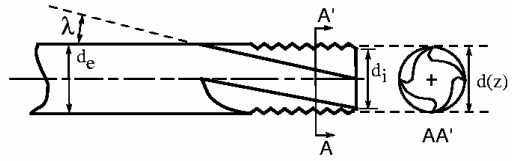

(b)

Figure 2. Tool and thread geometries (a)Thread geometry, (b) Tool geometry.

The thread milling tool is very similar to an end milling tool. The tool geometry of a helical thread flute is presented in Fig. 2b. The helix angle λ, the rake angle α (not shown in the figure), the internal and external diameters d_i and d_e and the number of flutes N_f define the tool geometry. The angle between the flutes is:

$$\zeta = \frac{2\pi}{N_f} \tag{2}$$

and the number of each flute is n, $1 \le n \le N_f$. The local diameter d(z) is written as a function of the height z, $d_i \le d(z) \le d_e$, calculated as follows:

$$d(z) = \begin{cases} d_i + \dfrac{2\left(z - nt(z)\dfrac{p}{2}\right)}{\tan(\xi/2)}, & \text{if } nt(z) \text{ is odd;} \\ d_e - \dfrac{2\left(z - nt(z)\dfrac{p}{2}\right)}{\tan(\xi/2)}, & \text{if } nt(z) \text{ is even;} \end{cases} \tag{3}$$

where nt(z) is:

$$nt(z) = \text{Integer Part}\left(\frac{2z}{p}\right) \tag{4}$$

The tool motion is circular in the plane normal to the tool-axis and linear in the direction of the tool-axis with a stationary workpiece to generate the thread. The workpiece is predrilled and the diameter of the hole is called d_h. The width of cut (or radial depth of cut) is e(z):

$$e(z) = \frac{d(z) - d_h}{2} \tag{5}$$

Cutting Geometry

The cutting geometry of the thread milling process is different than the common end milling because the cutting edge is not a straight line and the tool follows a circular trajectory. Following the approach used by Tlusty and MacNeil (1975) the contact interface in thread milling process can be described as shown in Fig. 3, where the depth of cut, b, can be observed.

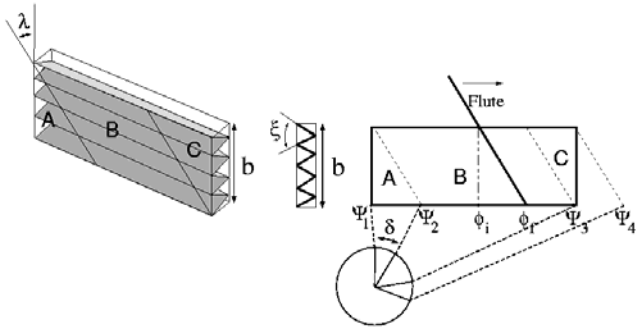

Figure 3. Contact phases.

The contact surface is divided in three phases: **A**, where the length of active cutting edge increases in time, **B**, where it is constant, and **C** where it decreases. There are two different types of contact surface geometry according to the relation between the angle δ, defined in Eq. (6), and the contact angle: *Type I* and *Type II*. It is a *Type I* geometry if $\delta \le \varphi_2$, and *Type II* occurs if $\delta \ge \varphi_2 - \varphi_1$.

$$\delta = \frac{2\,b\tan\lambda}{d_e} \tag{6}$$

The contact angle is defined as the difference between the initial angle φ_1 and the final angle φ_2. Two auxiliary angles were defined by Tlusty and MacNeil (1975) to analyze the flute movement through the three phases **A**, **B** and **C**. The first one is angle ψ, which indicates the angular position of the leading point of the cutting edge. The other one is angle ϕ, which indicates the position of the other points of the same flute. For a known ψ , the range of values

for ϕ is between ϕ_i and ϕ_f , and it changes for each phase and each position θ of the tool as shown in Table 1.

The range of values for ψ in each phase is shown on Table 2 and the limits of each phase are called ψ_1, ψ_2, ψ_3 and ψ_4 .

Table 1. Limits of $\phi_i(\theta)$ and $\phi_f(\theta)$ in A, B and C (Araujo and Silveira, 2001).

	Type I		Type II	
Phase	$\phi_i(\theta)$	$\phi_f(\theta)$	$\phi_i(\theta)$	$\phi_f(\theta)$
For $\psi_1 < \theta \le \psi_2$ - Phase A	φ_1	θ	φ_1	θ
For $\psi_2 < \theta \le \psi_3$ - Phase B	$\theta - \delta$	θ	φ_1	φ_2
For $\psi_3 < \theta \le \psi_4$ - Phase C	$\theta - \delta$	φ_2	$\theta - \delta$	φ_2

Table 2. Values of ψ_1 , ψ_2 , ψ_3 and ψ_4 for Type I and Type II.

	Type I	Type II
ψ_1	φ_1	φ_1
ψ_2	$\varphi_1 + \delta$	φ_2
ψ_3	φ_2	$\varphi_1 + \delta$
ψ_4	$\varphi_2 + \delta$	$\varphi_2 + \delta$

For a helical tool, the height z can be expressed as a function of the position of the tool θ and the point angle ϕ:

$$z(\theta,\phi) = \frac{d_i(\theta - \phi)}{2\tan\lambda} \tag{7}$$

In the case I, shown in Fig. 4a, the tool feed velocity does not change direction, as occurs in end milling. In case II the tool cuts in a the circular path, Fig. 4b.

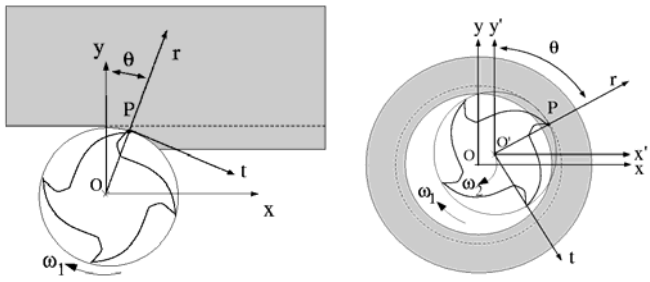

a) Case I **b) Case II**

Figure 4. Tool path cases.

Case I

For up milling the initial angle is zero. In case I the final angle is written as:

$$\varphi_2 = \frac{b\tan\lambda}{r\,.\,e} \tag{8}$$

Case II

In case II (Fig. 5), the final angle is written as:

$$\varphi_2 = \arcsin\left(\frac{d_h^2 - d_i^2 - 4r_o}{4d_h r_o}\right) \tag{9}$$

where $r_o = \dfrac{d_E - d_e}{2}$.

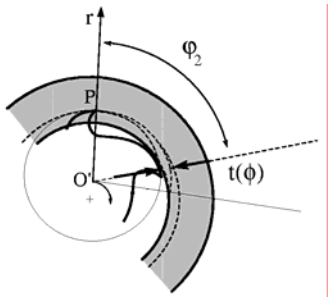

Figure 5. Chip thickness for case II.

The uncut chip thickness for any point of the cutting edge, located in the height z and by the angle ϕ (Fig. 5), can be written as (Sabberwall, 1960):

$$t(\phi, z) = f_t(z)\sin\phi \tag{10}$$

Force Prediction

Elemental normal and frictional forces are required to the determination of cutting forces for a given geometry. The mechanistic modelling approach is a combination of analytical and empirical methods in which the forces are proportional to the chip load (Kline and DeVor, 1983). The specific cutting energies, K_n , K_f and K_z , have been shown as a function of chip thickness t_c and cutting speed V_c (Dogra et al., 2002).

$$\begin{aligned} F_n(\theta) &= K_n A(\theta) \\ F_f(\theta) &= K_f A(\theta) \end{aligned} \tag{11}$$

$$\begin{aligned} \ln(K_n) &= a_0 + a_1\ln(t_c) + a_2\ln(V_c) + a_3\ln(t_c)\ln(V_c) \\ \ln(K_f) &= b_0 + b_1\ln(t_c) + b_2\ln(V_c) + b_3\ln(t_c)\ln(V_c) \end{aligned} \tag{12}$$

The coefficients a_0 , a_1 , a_2 , a_3 , b_0 , b_1 , b_2 and b_3 are called specific cutting energy coefficients. They are dependent on the tool and workpiece materials and also on the cutting speed and the chip thickness. They are determined from calibration tests for a given tool workpiece combination and for a given range of cutting conditions.

Chip Cross Area

The function of chip cross area for the first flute $A_1(\theta)$ is:

$$A_1(\theta) = \int_{\phi_i(\theta)}^{\phi_f(\theta)} t(\phi, z)\,db \tag{13}$$

where db is (Sabberwal, 1960):

$$db = \frac{d(z)}{2\tan\lambda}d\phi \tag{14}$$

Using the Eq. (3), Eq. (7) and Eq. (10), the area $A_1(\theta)$ can be calculated as:

$$A_1(\theta) = \int_{\phi_i(\theta)}^{\phi_f(\theta)} t(\phi, z(\theta,\phi))\frac{d(z(\theta,\phi))}{2\tan\lambda}d\phi \tag{15}$$

The limits $\phi_i(\theta)$ and $\phi_f(\theta)$ are functions of the θ and the cutting phase of θ, as shown in Table 1. In order to add the contributions of

all flutes, the chip cross-sectional area function for each flute (n) is written as:

$$A_n(\theta) = \int_{\phi_i(\theta+\zeta(n-1))}^{\phi_f(\theta+\zeta(n-1))} t(\phi, z(\theta,\phi)) \frac{d(z(\theta,\phi))}{2\tan\lambda} d\phi \qquad (16)$$

In Eq. (15) ϕ_i and ϕ_f are also written as a function of n.

The total area $A(\theta)$ is calculated as:

$$A(\theta) = \sum_{n=1}^{N_f} A_n(\theta) \qquad (17)$$

Tool Run Out

Cutter run out exists in all kinds of milling operations and results in variations in the undeformed chip thickness, local forces and machined surface characteristics. The run out can be due to cutter axis offset, eccentricity (ρ) or cutting points positioning offset (ε), shown in Fig. 6, and it depends principally on the characteristics of the spindle and tool holder. The chip thickness in presence of run out is rewritten as (Kline and DeVor, 1983):

$$t_c(\theta,\phi,n) = f_t \sin\phi + \rho(\cos(\theta - \varepsilon - \phi) - \cos(\theta - \varepsilon - \phi - n\zeta)) \qquad (18)$$

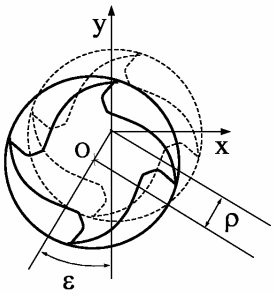

Figure 6. Tool run out (Kline and DeVor, 1983).

Force Computation

To calculate the components of the cutting forces using the specific cutting forces K_f , K_n and K_z, a function $A_R(\theta)$ has to be introduced (Araujo and Silveira, 2001).

$$F(\theta) = \begin{bmatrix} F_{x'}(\theta) \\ F_{y'}(\theta) \\ F_{z'}(\theta) \end{bmatrix} = \begin{bmatrix} F_x(\theta) \\ F_y(\theta) \\ F_z(\theta) \end{bmatrix} = A(\theta) \begin{bmatrix} K_x \\ K_y \\ K_z \end{bmatrix} = A_R(\theta) \begin{bmatrix} K_f \\ K_n \\ K_z \end{bmatrix} \qquad (19)$$

In fact, the function $A_R(\theta)$ is the rotation matrix $R(\theta)$ multiplied by the area.

$$R(\theta) = \begin{bmatrix} \cos(\theta) & \sin(\theta) & 0 \\ \sin(\theta) & -\cos(\theta) & 0 \\ 0 & 0 & 1 \end{bmatrix} \qquad (20)$$

For each flute the rotation matrix $R_n(\theta)$ is:

$$R_n(\theta) = \begin{bmatrix} \cos(\theta+\zeta(n-1)) & \sin(\theta+\zeta(n-1)) & 0 \\ \sin(\theta+\zeta(n-1)) & -\cos(\theta+\zeta(n-1)) & 0 \\ 0 & 0 & 1 \end{bmatrix} \qquad (21)$$

The area for all flutes is written as:

$$A_R(\theta) = \sum_{n=1}^{N_f} R_n(\theta) A_n(\theta) \qquad (22)$$

Examples

In order to analyze the forces profile in thread milling, four examples are presented in this article. Specific pressure in these examples will be the same and are given by K_f = 900 N/mm^2, K_n = 500 N/mm^2 and K_z = 100 N/mm^2.

The tool used in the simulation has the following parameters: p=1.5 mm, $\lambda = 30^o$, $N_f = 4$ and $\xi = 60^o$. The geometry of cut and the velocities are: d_E = 10 mm, ω = 1400 rpm, f_t = 0.06 mm. The values for eccentricity and off set for the run out case are: ρ = 0.04 mm and $\varepsilon = 10^o$.

Example I

In this example the depth of cut is b = 1.5 mm, just one pitch. To illustrate the example I, Fig. 7 presents the chip cross area and the cutting force with and without tool run out.

Example II

The depth of cut in this example is b = 5 mm. Figure 8 presents the chip cross area and the cutting force with and without tool run out for this case.

Example III

In this example the depth of cut is b = 10 mm and Fig. 9 presents the chip cross area and the cutting force with and without tool run out for this example.

Example IV

In example IV the depth of cut is b = 20 mm. The chip cross area and the cutting force with and without tool run out for this example are presented in Fig. 10.

Conclusions

A mechanistic model have been developed for thread milling. The model takes into account the thread cutting edge and the linear movement of the tool. The forces were predicted for four depths of cuts. The results show the effects of the increasing the depth of cut on the cutting forces. The thready flute contribute for another frequency oscillation in chip cross area and consequently in cutting forces as compared to the straight cutting edge. In order to improve the model, the contact stresses between the threads and the tool need to be added.

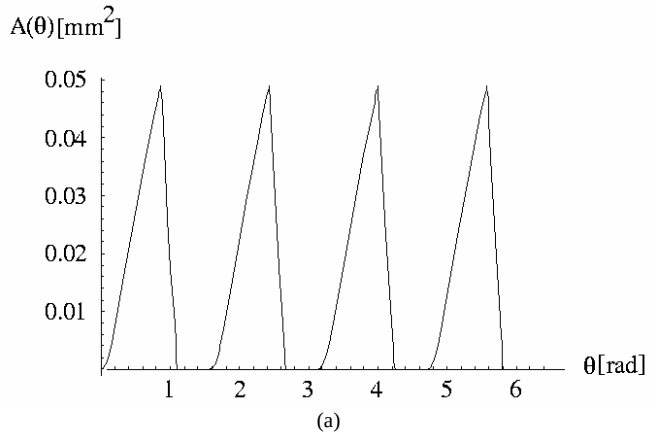

(a)

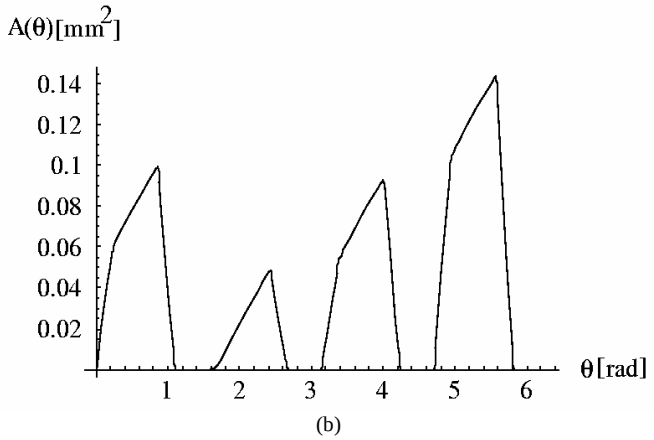

(b)

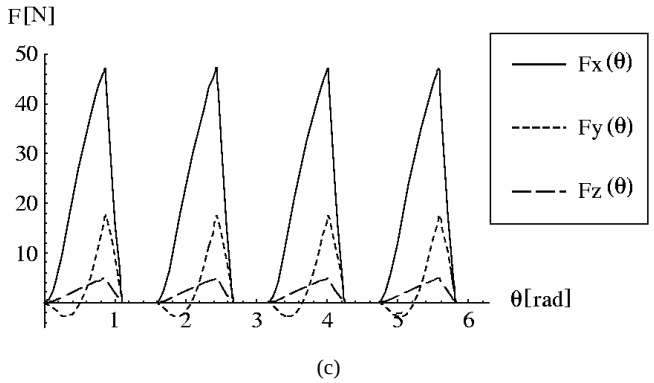

(c)

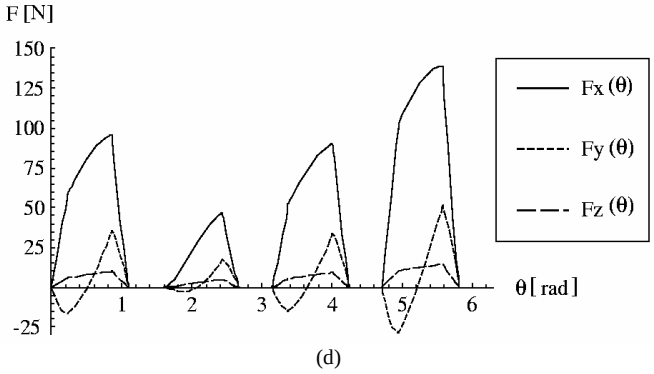

(d)

Figure 7. Example I. (a) Chip cross area, (b) Chip cross area with run out, (c) Cutting forces, (d) Cutting forces with run out.

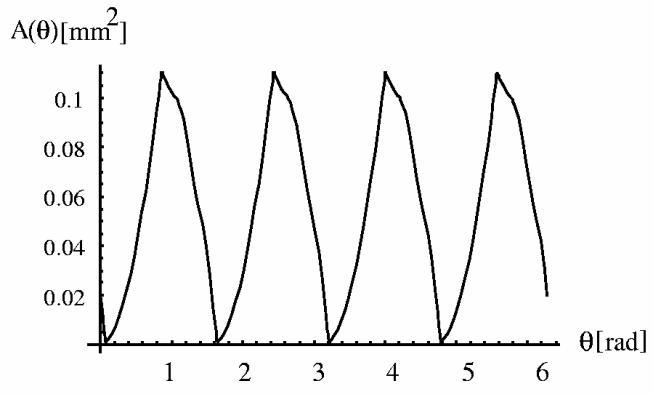

(a)

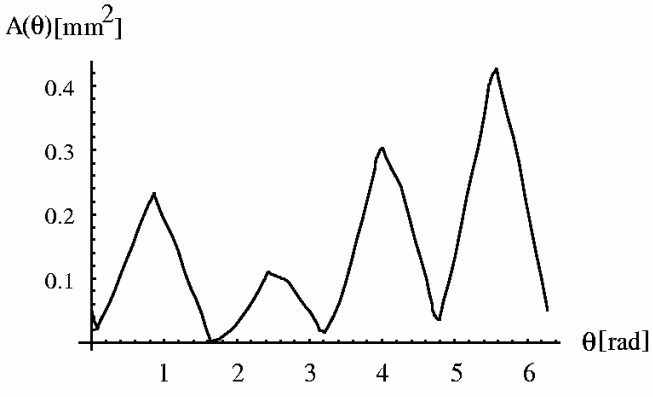

(b)

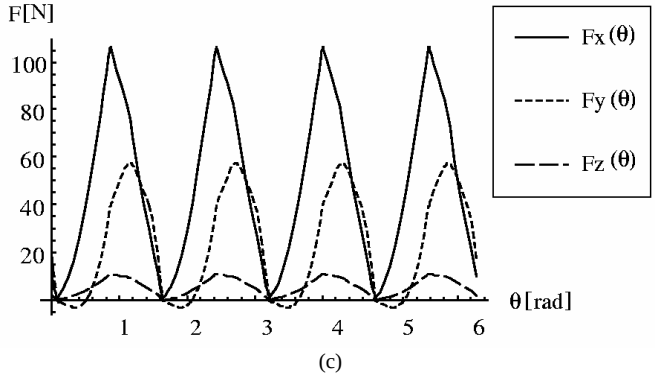

(c)

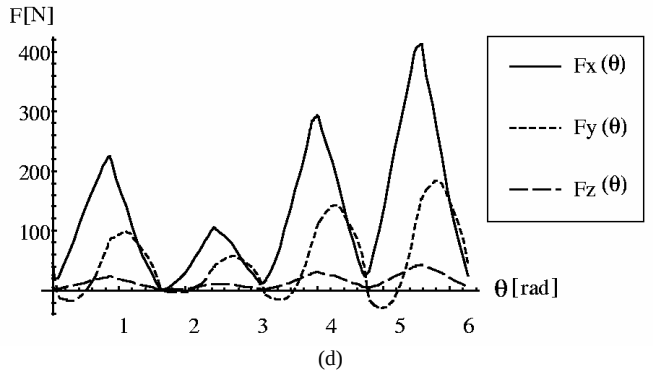

(d)

Figure 8. Example II. (a) Chip cross area, (b) Chip cross area with run out, (c) Cutting forces, (d) Cutting forces with run out.

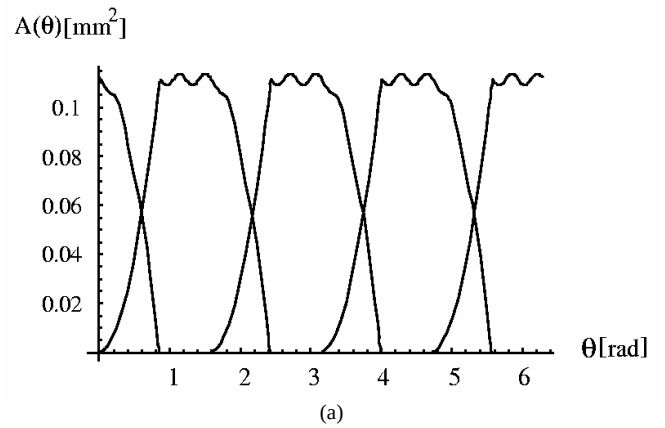

(a)

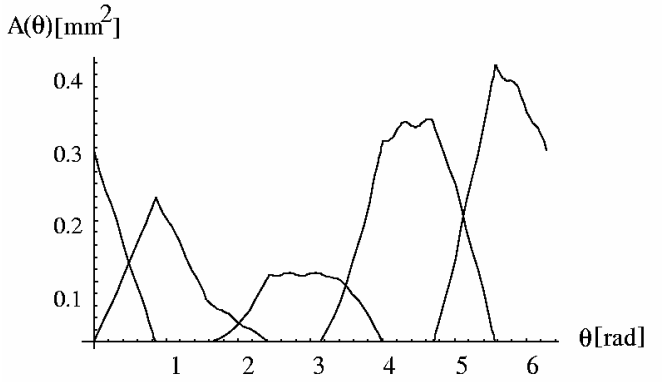

(b)

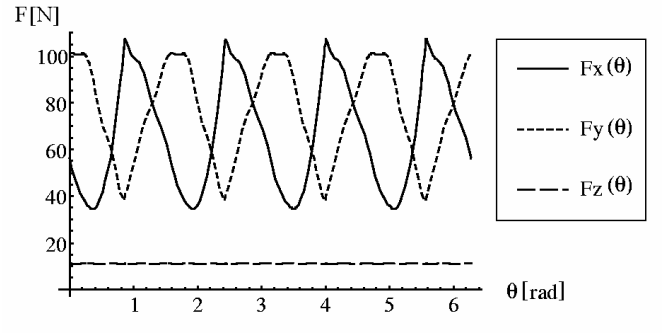

(c)

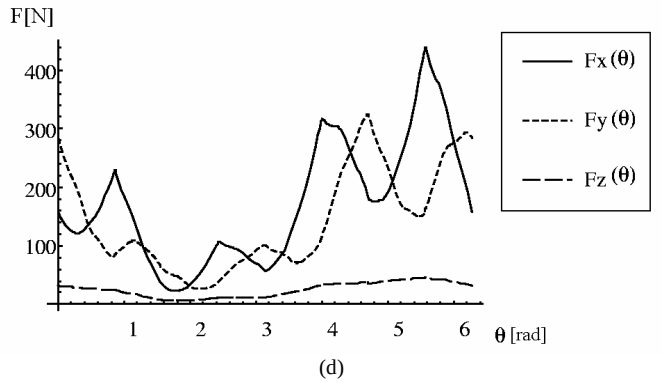

(d)

Figure 9. Example III. (a) Chip cross area, (b) Chip cross area with run out, (c) Cutting forces, (d) Cutting forces with run out.

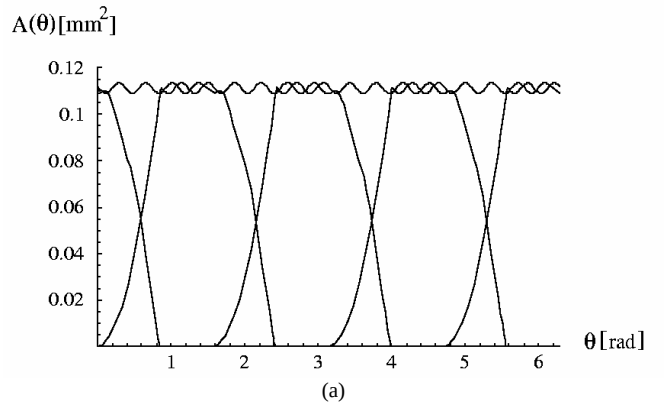

(a)

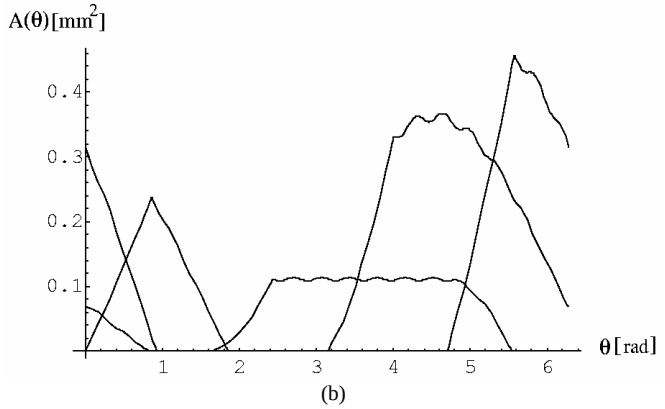

(b)

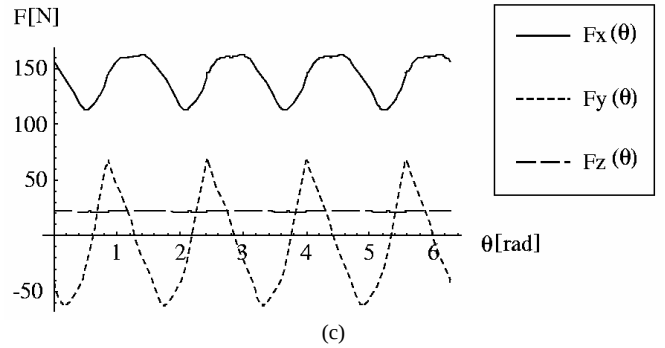

(c)

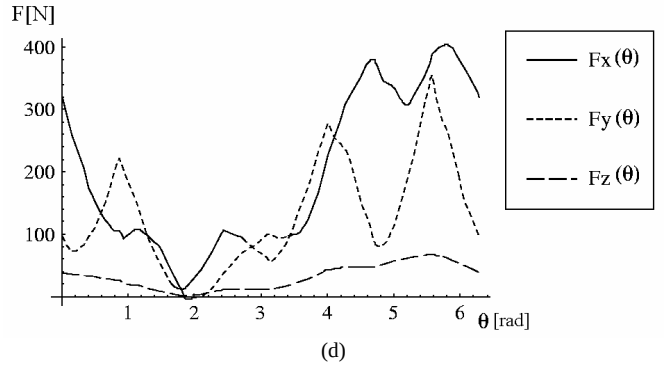

(d)

Figure 10. Example IV. (a) Chip cross area, (b) Chip cross area with run out, (c) Cutting forces, (d) Cutting forces with run out.

Acknowledgements

This project is fulfilled with the fellowship grant received from CNPq, a Brazilian council for scientific and technological development. The authors are grateful for the council and the University of Illinois at Urbana Champaign for the support.

References

Araujo, A.C. and Silveira, J.L., 2001, "The Influence of the Specific Cutting Force on End Milling Models", Proceedings of the 16th Brazilian Congress of Mechanical Engineering, CD-Rom, Uberlândia, MG, Brazil.

Dogra, A.P.S., Kapoor, S.G. and DeVor, R.E., 2002, "Mechanistic Model for Tapping Process with Emphasis on Process Faults and Hole Geometry", Journal of Manufacturing Science and Engineering, Vol. 124, pp.18-25.

Ehmann, K.F., Kapoor, S.G., DeVor, R.E. and Lasoglu, I., 1997, "Machining Process Modeling: A Review", Journal of Manufacturing Science and Engineering, Vol. 119, pp. 655-663.

Emuge Catalogs, 2002.

Smith, G., 1989, "Advanced Machining: The Handbook of Cutting Technology", IFS Publications, UK.

Kline, W.A., DeVor, R.E., 1983, "The Effects of Run-Out on Cutting Geometry and Forces in End Milling" International Journal of Machine Tool Design and Research, Vol. 23, pp.123-140.

Koelsch, J.R., Oct. 1995, "Thread Milling Takes on Tapping", Manufacturing Engineering.

Sabberwall, 1960, "Chip Section and Cutting Force During the Milling Operation", Annals of the CIRP, pp. 197-203.

Stephenson, D.A. and Agapiou, J.S., 1996, "Metal Cutting Theory and Practice", Marcel Dekker, Inc. New York, NY.

Tlusty, J. and MacNeil, 1975, "Dynamics of Cutting in End Milling", Annals of the CIRP, Vol. 24/1, pp. 213-221.